Available online at www.sciencedirect.com
SCIENCE DIRECT®
Earth and Planetary Science Letters 243 (2006) 229–243
EPSL
www.elsevier.com/locate/epsl

Pleistocene deglaciation chronology of the Amery Oasis and Radok Lake, northern Prince Charles Mountains, Antarctica

David Fink [a,*], Barrie McKelvey [b], Michael J. Hambrey [c], Derek Fabel [d], Roderick Brown [d]

[a] *Australian Nuclear Science and Technology Organisation, PMB 1, Menai, NSW 2234, Australia*
[b] *Earth Sciences, University of New England, Armidale, NSW 3251, Australia*
[c] *Centre for Glaciology, University of Wales, Aberystwyth, SY23 3DB, UK*
[d] *Department of Geographical and Earth Sciences, Glasgow University, Glasgow, G12 8QQ, UK*

Received 27 April 2005; received in revised form 2 December 2005; accepted 9 December 2005
Available online 10 February 2006
Editor: K. Farley

Abstract

The East Antarctic Ice Sheet is the largest ice mass on Earth with a capacity to raise global sea level by up to 65 m. As the Lambert Glacier–Amery Ice Shelf drainage system is the largest to reach the coast of Antarctica, quantifying its evolution over the Quaternary is a vital component in developing an understanding of the Antarctic response to future climate change. Here we present a deglaciation chronology based on ^{10}Be and ^{26}Al in situ cosmogenic exposure ages of the northern Prince Charles Mountains, which flank the Lambert Glacier–Amery system, and that records the progressive emergence of McLeod Massif and Radok Lake basin from beneath the Mac.Robertson Land lobe of the East Antarctic Ice Sheet. The exposure ages monotonically decrease with both decreasing altitude and increasing proximity to the Amery Ice Shelf at the Antarctic coast. Exposure ages from the crests of McLeod Massif near the edge the Amery Ice Shelf and from Fisher Massif, 75 km further inland, each at ~1200 m above sea level, are 2.2±0.3 and 1.9±0.2 Ma, respectively, suggesting their continuous exposure above the ice sheet at least since close to the Plio–Pleistocene boundary. An extensive plateau at ~800 m altitude on McLeod Massif above Battye Glacier records the massif's increased emergence above the ice sheet surface at about between 880 and 930 ka ago indicating 400 m of ice volume reduction in the mid Pleistocene. Correcting these apparent ages for a reasonable choice in erosion rate would extend this event to ~1.15 Ma — a period identified from Prydz Bay ODP core-1167 when sedimentation composition alters and rates decrease 10-fold. Exposure ages from boulder-mantled erosional surfaces above and beyond the northern end of Radok Lake at 220 m, range from 28 to 121 ka. Independent of choice of model interpretation to explain this age spread, the most recent major reoccupation of Radok Lake by Battye Glacier ice occurred during the last glacial cycle. Moraine ridges at the lower altitude of 70–125 m were deposited during the final withdrawal of Battye Glacier ice from the lake basin between 11 and 20 ka ago. This new chronology indicates that the highest Amery Oasis peaks have not been overridden by the Mac.Robertson Land lobe of the East Antarctic Ice Sheet for at least the past 2 Ma. Since this time we document 3 major periods of regional reduction in ice sheet volume at ~1.1 Ma, during the last glacial cycle (120 to

* Corresponding author. Tel: +61 2 9717 3048; fax: +61 2 9717 3257.
E-mail address: fink@ansto.gov.au (D. Fink).

0012-821X/$ - see front matter
doi:10.1016/j.epsl.2005.12.006

30 ka) and through the Last Glacial Maximum (20 to 10 ka) that resulted in an overall 1000 m of ice lowering in the Battye Glacier–Radok Lake region.

Keywords: Pleistocene glacial chronology; cosmogenic isotopes; northern Prince Charles Mountains; East Antarctic Ice Sheet

1. Introduction

The Antarctic ice sheets have a fundamental influence on world wide sea level change, oceanographic processes and global climate. Yet their evolution and dynamics through the Neogene and Pleistocene, and particularly that of the larger East Antarctic Ice Sheet (EAIS), are not well understood. This situation is slowly changing with the advent of cosmogenic surface exposure age dating that provides a geochronological framework to underpin glacial geological field observations. Cosmogenic exposure dating, based on ^{10}Be, ^{3}He and ^{21}Ne, in the Dry Valleys of the Transantarctic Mountains [1–6] have been convincingly employed to determine the age of uplifted Sirius Group strata in an attempt to address the controversial issue of EAIS Plio–Pleistocene stability [7–11]. Cosmogenic ages from sites further afield, such as in the Sør Rondane Mountains [1], the Shackleton Range [12] and in North Victoria Land [13], have been similarly used to establish the persistence in these localities of a cold hyper-arid Antarctic climate and landscape preservation since at least the early Pliocene. However, extension of such a conclusion to cover the whole of the East Antarctic ice sheet requires further cosmogenic chronological studies in other ice-free regions, particularly at locations adjacent to major drainage systems of the ice sheet. Exposure ages from ice-proximal locations goes far to validate the interpretation of proxy climatic records from off-shore ocean sediment cores and to constrain ice limits for climatic episodes identified from ice cores. Our aim is to provide constraints on the nature and timing of Pliocene–Quaternary glacial events and relative ice-thickness changes in the region to document the long-term evolution of the EAIS and the complex interplay with peripheral alpine glacier mountain systems.

We report here on the first set of paired ^{10}Be and ^{26}Al in situ cosmogenic exposure ages of erratics and bedrock surfaces from the Amery Oasis in the northern Prince Charles Mountains (PCMs) which borders the western flank of the vast 80 km wide and 550 km long Lambert Glacier–Amery Ice Shelf (LG–AIS) system. This drainage system and the numerous alpine glacier systems throughout the PCMs conveys ca. 10% by surface area of the EAIS into Prydz Bay (Fig. 1). We focus attention on the Radok Lake basin and Battye Glacier adjacent to McLeod Massif in the Amery Oasis (Figs. 2,3), and on Fisher Massif, 75 km further inland (Fig. 1). Our Amery Oasis sample sites pertain more to the ice history of coastal regions within the LG-AIS drainage system and thus we are aware our chronological interpretation may not be fully representative of the system as a whole. In particular we remain cautious when comparing and attempting to integrate our data sets with those available from the Trans-Antarctic Mts, Dry Valleys and elsewhere in Antarctica, such as those presented by Stone et al. [14] in their study of the thinning West Antarctic Ice Sheet. The present results are the first of an ongoing program by ourselves and other workers to obtain more data sets throughout not only the northern PCMs, but also the Mawson Escarpment, Mt Menzies and other nunataks [15] including those deepest south such as Komsomol'skiy Peak and the Grove Mountains [16].

2. Physiographic setting

The Amery Oasis (Fig. 2) covers an area of ~1800 km^2 [17] and is largely ice-free. Radok Lake basin (Fig. 3) in the southern part of Amery Oasis lies between the rugged McLeod Massif to the west and much lower terrain, including Dart Fields and Flagstone Bench, to the east. The lake is 10 km long and more than 346 m deep [17,18]. Its ice-covered surface is ~7 m above sea level (masl). The lake drains eastwards via Bainmedart Cove and the 7-km long Pagodroma Gorge into the much larger Beaver Lake basin. Battye Glacier flows from the Mac.Robertson Land lobe of the EAIS at ~1000–1200 masl eastwards down into Radok Lake, and extends out across it for 2 km as a floating ice tongue (Fig. 3).

Geologically, Amery Oasis lies on the western shoulder of the Lambert Graben [19] along which flows the LG–AIS drainage system [20]. McLeod Massif to the west of Radok Lake is composed largely of Proterozoic gneisses and granulites [21]. The Amery Fault, co-incident with the axis of Radok Lake, separates the western Proterozoic basement from the Permo–Triassic fluvial Amery Group to the east [22]

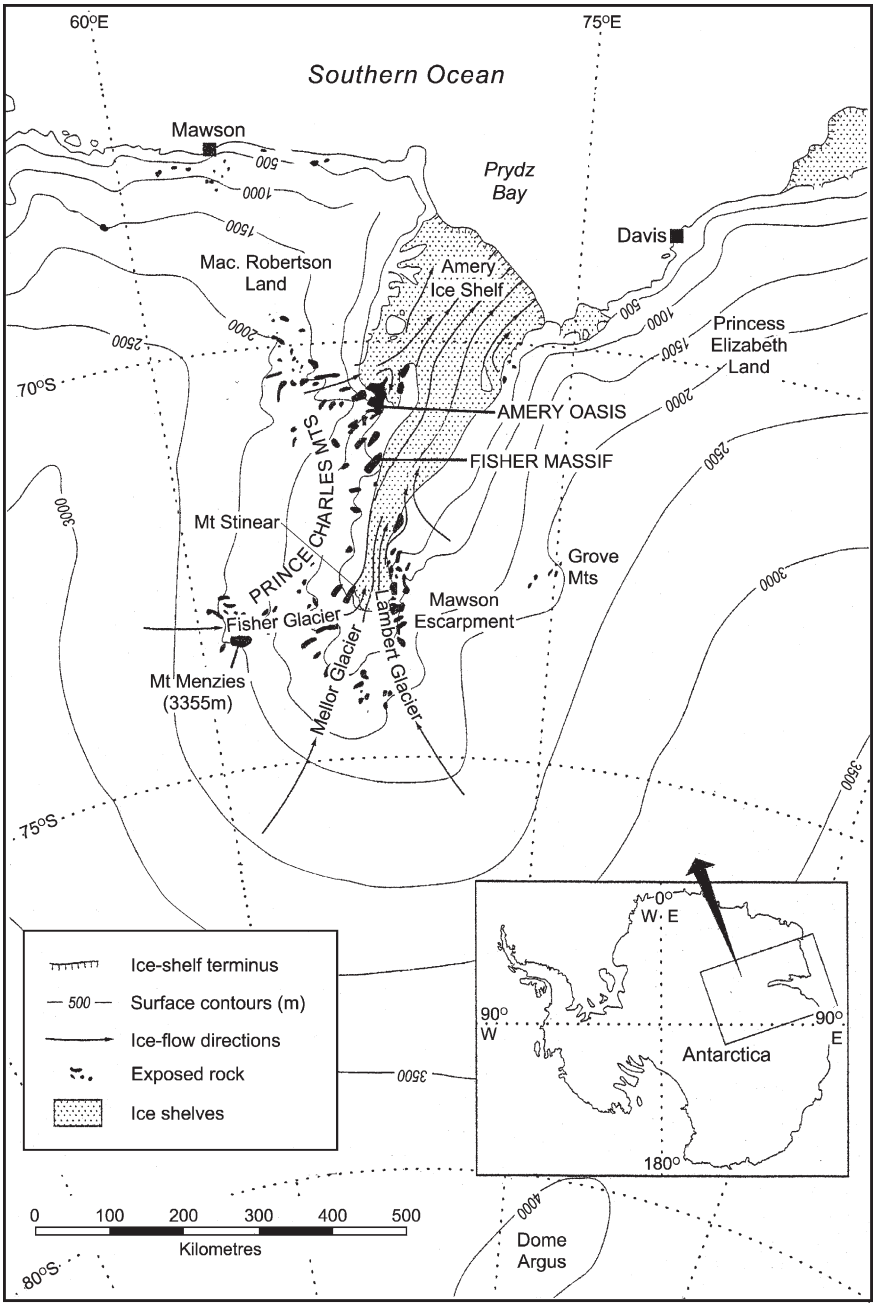

Fig. 1. Setting of Amery Oasis and Fisher Massif on western flanks of the Lambert Glacier–Amery Ice Shelf drainage system, showing flow lines through the system. Map based on Fig. 1 from Hambrey and McKelvey [25]. Two samples for cosmogenic dating were taken from the peak of Fisher Massif and the remaining 15 from Mcleod Massif and Radok Lake in Amery Oasis. Inset locates the geographic setting within Antarctica.

and which also extends into the Beaver Lake basin (Figs. 2 and 3). An irregular blanket of Neogene glacial strata, consisting of two formations of the glaciomarine fjordal Cenozoic Pagodroma Group [23–26], irregularly mantles much of the southern Amery Oasis and other ranges and nunataks of the northern PCMs. These strata were deposited during major episodes of ice sheet contraction, when the consequent recession of the LG–AIS drainage system allowed deep incursion of Southern Ocean waters to as far as 400 km inland. Subsequent uplift during later expansions of the drainage system, preserved erosional remnants of the Pagodroma Group in sequences up to 400 m thick on the mountains.

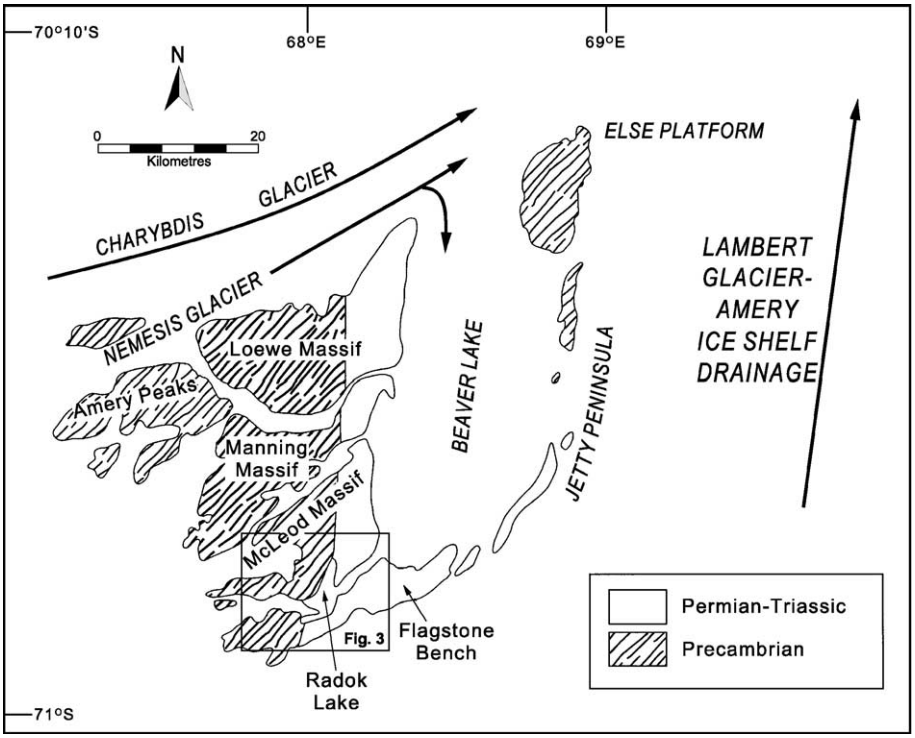

Fig. 2. Sketch map of the Amery Oasis, northern Prince Charles Mountains. Adapted from Fig. 3 of McKelvey et al. [23]. The boxed inset locates area of the sampling region at McLeod Massif and Radok Lake. Further details are given in Fig. 3 of this work.

High above the western shore of Radok Lake, along the Dragons Teeth, the mid-Miocene Battye Glacier Formation [23] of the Pagodroma Group overlies the Proterozoic basement and is itself in places overlain by thin glacigene Pleistocene gravels and felsenmeer. East of the lake, the Pliocene–early Pleistocene Bardin Bluffs Formation [24] blankets much of the Amery Group. Since deposition a minimum uplift in the order of 180 m is demonstrated by the highest surviving outcrops of the Bardin Bluffs Formation overlooking the northern shore of Radok Lake and on Flagstone Bench (Fig. 3).

Whereas the Pagodroma Group records the Neogene glacial and uplift histories of the northern PCMs, the late Quaternary to Holocene glacial history and geomorphic development of the post-Pagodroma Group at Amery Oasis is less well documented with the exception of works by Adamson et al. [17] and Bardin [18]. Even cursory observations suggest an intricate and as yet little understood history. Adamson et al. [17] considered Radok Lake to have existed in its present form for much of the late Quaternary, and its excavation by the Battye Glacier was during periods of colder climate following the deposition of the mid-Miocene Battye Glacier Formation. Both the North Arm and Bainmedart Cove reaches of Radok Lake were excavated by the glacier. Along the northeastern shore of North Arm, traces of former shorelines exist preserved up to 80 m above the present lake surface (see fig. 6 in [17]).

Prominent thrust moraines at 70–120 m distributed above the northern shore of North Arm were emplaced by northwards flowing Battye Glacier ice [17]. Similar and presumably contemporaneous thrust moraines also occur towards the head of Bainmedart Cove at the uppermost reach of Pagodroma Gorge, and at the southern shore of Radok Lake (see fig. 2b in [26]). The North Arm thrust–moraine complex contrasts with the much more subdued glacial deposits at higher elevation extending further to the north (Fig. 3) which were deposited by an older phase of Battye Glacier following the initial excavation of Radok Lake. Adamson et al. [17] considered neither Beaver or Radok lakes to have been overridden by an erosive ice stream since deposition of the Plio–Pleistocene Bardin Bluffs Formation. They emphasize that an ice-covered ridge effectively blocks the eastern and southern margins of the Amery oasis from the current LG–AIS drainage system with the Lambert Glacier flowing then, as it does today, around and not over the oasis.

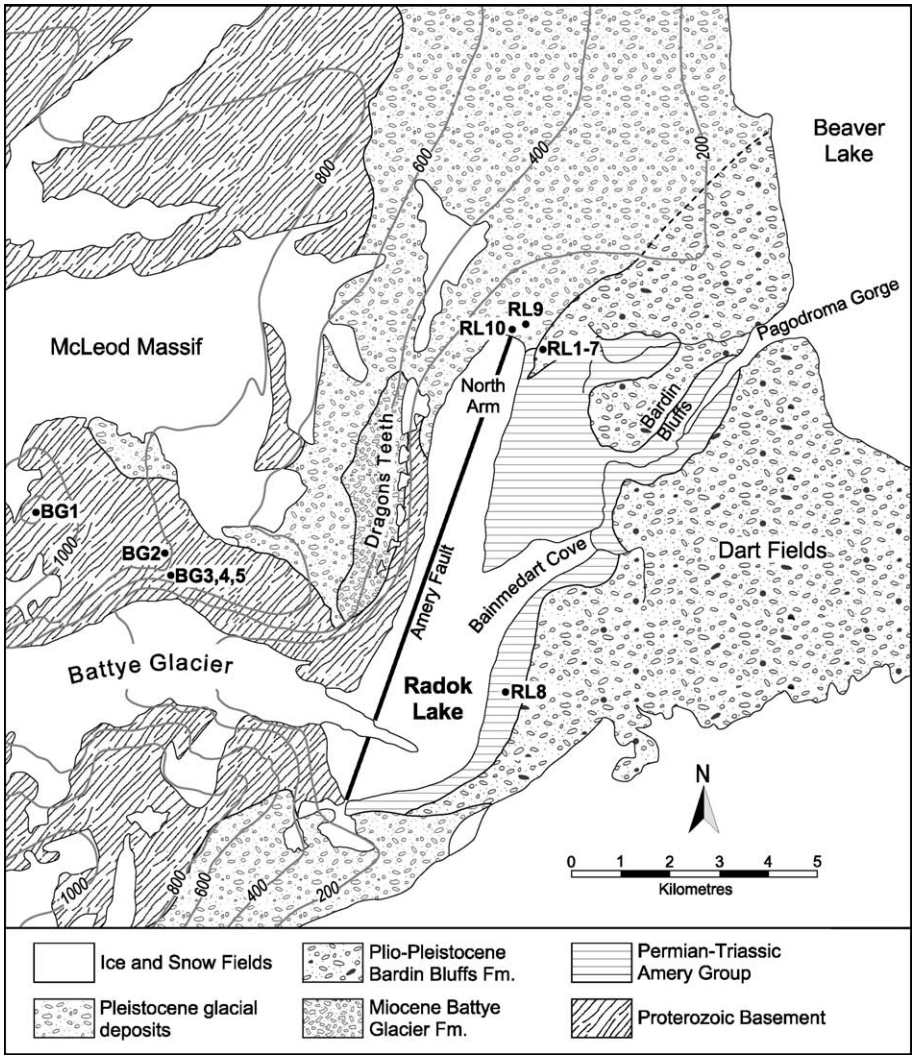

Fig. 3. Relevant physiographical and geological features of the McLeod Massif–Radok Lake basin region of the Amery Oasis indicating locations of erratic and bedrock sample sites for this study, numbered according to Tables 1 and 2.

Ocean sediment records form ODP cores in Prydz Bay exhibit a complex and extensive record of Lambert Glacier ice volume fluctuations. Hambrey et al. [27] described the Cenozoic sedimentary record (ODP Leg 119) spanning the last 35 My and conclude that approximately 60% of Lambert–Amery system ice entering Prydz Bay during the Plio–Pleistocene period is of near coastal derivation. The younger Pleistocene sedimentary record obtained from ODP Leg 188, Site 1167 [28], shows (1) a major shift in both sediment composition and a reduction in accumulation rates occurring at ~1.1 Ma and (2) that extensive advances of the LG–AIS system to the continental shelf abated during mid-late Pleistocene indicating a reduction in delivery of Lambert ice or over-deepening of the Lambert–Amery basin.

3. Sample collection and description

During the Australian National Antarctic Expedition 1994/1995 field season to the northern PCMs, 17 samples were collected for cosmogenic exposure dating from the Amery Oasis and Fisher Massif (see Table 1). Three locations in particular were sampled (see Figs. 1 and 3): (i) the summit of Blustery Cliffs at the northern end of Fisher Massif (FM-1 and -2), (ii) the summit of McLeod Massif (BG-1), and a gentle sloping plateau adjacent to the escarpment directly overlooking Battye Glacier (BG-2 to BG-5) and (iii) above the northern and

Table 1
Sample description, $^{10}Be/Be$ and $^{26}Al/Al$ AMS ratios, and relevant data

	Sample name[a]	Sample description	Altitude (masl)	$^{10}Be/Be$ ($\times10^{-15}$)[b]	$^{26}Al/Al$ ($\times10^{-15}$)[b]	Be mass (mg)[c]	Al conc. (ppm)[d]	Quartz mass (g)
Fisher Massif (71.26° S, 67.7° E)								
1	FM-1	Fisher summit, Blustery Cliffs; granite bedrock	1260	10,130±60	58,170±990	0.982	43.1[#]	24.51
	FM-1-R	Full repeat sample		11,390±60	43,510±500	0.359	35.2[#]	10.20
2	FM-2	Fisher summit, quartz vein on tor	1187	2120±40	75,720±2120	1.011	31.1	15.33
	FM-2-E	Repeat etch		1910±15	NA	1.036		14.60
Battye Glacier (70.50° S, 67.6° E)								
3	BG-1	McLeod Massif summit, 0.5 m granite tor on pavement	1200	8640±70	NA	1.488		35.91
4	BG-2	Erratic (L×W)×H=(4×3)×1.5 m	803	4040±120	NA	1.503		40.00
5	BG-3	Granite tor (~2 m) on erosional surface	782	3775±80	NA	0.706		18.66
	BG-3-E	Repeat etch		3160±45	NA	1.517		34.28
6	BG-4	Erratic in fossil river bed (0.5×0.5)×0.5 m	771	3600±70	12,600±230	0.701	NA	22.10
	BG-4-R	Full repeat sample	771	11,480±150	13,660±185	0.700	109.3	70.82
7	BG-5	Erratic in fossil river bed (0.5×0.5)×0.5 m	771	1970±50	NA	1.251		25.44
Radok Lake (70.48° S, 68.0° E)								
8	RL-1	Erratic (10×10)×4 m	216	191.4±5.2	2360±215	1.251	47.2	30.87
9	RL-2	Erratic (2×2)×2 m	212	590.0±11.1	3355±80	0.773	73.5	44.80
10	RL-3	Erratic (small)	212	1402±19.5	3485±111	0.766	139.0	80.21
11	RL-4	Erratic (2×1)×1 m	203	232.2±10.6	288±27	0.683	405.4	50.59
12	RL-5	Bedrock sample	197	526.8±30.6	NA	0.815		33.67
13	RL-6	Erratic cobble (0.2×0.1×0.1 m)	197	566.8±22.4	NA	0.811		40.84
14	RL-7	Erratic (1×1.5)×0.5 m	197	101.9±13.0	NA	0.831		27.67
15	RL-8	Striated sandstone bedrock (70.52 S)	125	105.3±3.3	227±30	0.856	127.7	55.80
16	RL-9A	Erratic (4×5)×2 m	123	75.7±5.0	329±35	0.702	104.4	23.90
	RL-9B	Opposite corner from RL-9A of sample 16	123	81.1±7.8	429±33	0.761	92.9	29.88
17	RL-10	Sandstone erratic (1×1)×1 m	70	85.0±4.5	230±19	0.690	62.4[#]	53.72

[a] 'E' denotes repeat analyses of a quartz powder aliquot after additional HF etching steps. 'R' denotes repeat analyses commencing from untreated crushed rock. Samples RL-9A and -9B from the same boulder but from diagonally opposite corners. All samples were granodiorites apart from FM-2, quartz, and RL-8 and RL-10, sandstones.

[b] Final AMS isotopic ratio determined after chemistry blank subtraction and normalization to AMS standards in use at the ANTARES AMS facility (PRIME-Z-9203 for $^{26}Al/Al$, nominal value=16,800×10^{-15}; NIST-3425 for $^{10}Be/Be$, nominal value=30,200×10^{-15}; see text).). Blanks prepared from commercially purchased 1000 ppm Be and Al standard solutions. Independent AMS measurements ($n>3$ repeats) were combined as weighted means with the larger of the total statistical error or mean standard error.

[c] Be carrier determined by mass from an ICP (MERCK) calibration solution at 1000±3 ppm (mg/L).

[d] Al concentration measured by ICP-AES. A representative error of ±4% is assigned to all ICP results. [#]Samples FM-1, FM-1-R and RL-10 were processed with 1.011, 0.641 and 0.977 mg Al carrier.

northeastern shores of Radok Lake (RL-1 to RL-10). Samples, RL-1 to -7 were clustered in close vicinity at an elevation of ~200 m above the North Arm of Radok Lake, while samples RL-9 and -10 are from the thrust moraines referred to above and at lower altitude approximately 1 km distant from the previous site. Sample RL-8 is from above the southeastern shore of Radok Lake. All samples were taken from either bedrock outcrops (FM-1, -2, BG-1, -3, and RL-5, -8) or boulders in diamict of the Pagodroma Group, or alternatively from the crests of erratics. In view of the open character of the landscape, corrections for cosmic ray shielding from horizon obstructions were not necessary.

4. AMS results and in situ cosmogenic methods

Rock samples were processed for ^{10}Be and ^{26}Al from quartz following procedures outlined in [29] and modified by Child et al. [30]. Sample thickness was restricted in most cases to <4 cm surface slices. AMS measurements were carried out at the ANTARES AMS Facility at ANSTO, Australia [31] using methods described by Fink et al [32]. Measured $^{10}Be/^{9}Be$ and $^{26}Al/Al$ ratios (see Table 1) were corrected by full chemistry procedural blanks, $<10\times10^{-15}$ and $<5\times10^{-15}$, respectively. Final analytical error in concentrations (atoms/g quartz) are derived from a quadrature sum of the standard mean error in an AMS ratio, 2% for

AMS standard reproducibility, 1% in Be spike assay, and 4% error in the ICP-AES Al quartz concentration. These range from 2% to 5% for ^{10}Be atoms/g and 5–9% for ^{26}Al atoms/g.

Currently there is considerable uncertainty as to the correct value for the ^{10}Be half-life [33,34] which is directly reflected in the debate surrounding the quoted (and certified) ^{10}Be/^{9}Be atom ratio issued by the National Institute of Standards and Technology (NIST, Gaithersburg, MD, USA) for ^{10}Be standard reference material (SRM) NIST-4325 [35,36]. Aside from the course of events which led to this circumstance and attempts to re-determine the ^{10}Be half-life [37,38], no definitive resolution has emerged. The NIST-4325 ^{10}Be SRM is employed for normalization of all measured ^{10}Be/^{9}Be ratios at ANTARES. However we have chosen not to use the certified NIST-4325 SRM ^{10}Be/^{9}Be isotope ratio but a value of $30{,}200\times10^{-15}$ derived by renormalizing the NIST-4325 value upwards by 1.127, which is equivalent to the ratio of the NIST ^{10}Be half-life (1.34 Ma) [35] to that commonly in use (1.51 Ma) [37,38]. To ensure self-consistency with the above procedure, we convert all AMS-derived ^{10}Be concentrations to exposure ages using a ^{10}Be half-life of 1.51 Ma, (while for ^{26}Al, a half-life of 0.70 Ma was used) — these being the values employed in determination of the nominal AMS ratios for the standards in use at ANTARES.

To calculate apparent exposure ages, we employed the standard models of Lal [39] with sea-level high latitude (>60°) nuclide production rates of 5.1± 0.3 atoms g^{-1} yr^{-1} (^{10}Be) and 31.1±1.9 atoms g^{-1} yr^{-1} (^{26}Al) scaled to altitude and latitude using algorithms specific for the Antarctic region by Stone [40]. Altitude scaling according to methods described by Dunai [41] (using the same adiabatic lapse rate and surface temperature) results in exposure ages only 2–4% younger. Table 2 lists samples in decreasing altitude, with cosmogenic radioisotope concentrations, production rates, scaling factors, and *minimum* exposure ages with associated errors.

Uncertainties in single-nuclide exposure ages represent propagation of all concentration errors defined above in quadrature with production rate uncertainties of 7%. Exposure age corrections due to production rate variations as a function of changes in the paleogeomagnetic dipole intensity are not required for latitudes greater than about >55°. Our procedures to renormalize absolute ^{10}Be concentrations and quote ages based on the 1.51 Ma half-life (as discussed above) requires some careful attention. Recalculating all ages based on a 1.34 Ma half-life and the reported NIST-4325 ^{10}Be concentration, which in principle is also a self-consistent operation, interestingly does not result in a constant scaling of all ages downwards by the ratio of the new-to-old half-life. This is due to the fact that one must also modify the sea-level high-latitude production rate of 5.1 atoms/g/yr [40] downwards by the same factor as this production rate had been originally extracted on the implicit assumption of a 1.51 Ma ^{10}Be half-life for AMS standards used by Nishiizumi et al. [42]. Had we chosen alternatively to use the NIST-4325 certified values (half-life and concentration), the change in final exposure age from those ages given in Table 2 (based on a 1.5 Ma ^{10}Be half-life) is negligible for ages <200 ka, a 3% increase for ages <0.8 Ma and a shift of +9% for those samples at 2 Ma.

A number of repeat procedures were carried out to gauge reliability and reproducibility in age determinations. Two samples, FM-1 and BG-4, underwent complete reprocessing starting from crushed rock powder. The repeat ^{10}Be concentrations agreed remarkably well to within <2%. Two other samples, FM-2-E and BG-3-E, underwent additional HF etching stages during sample processing in order to evaluate age dependency on the degree of quartz etch. Again in both cases, ^{10}Be concentrations were reproduced to better than 5%. Sample RL-9, a very large granulite boulder (4×5 m in horizontal section, 2 m in height), was sampled at diametrically opposite corners, (i.e. RL-9A and RL-9B). The paired ^{10}Be and ^{26}Al results for each are well within their 1-σ errors.

Ages listed in Table 2 do not include the effect of erosion of the sampled rock surface. However we have no *independent* means by which to estimate an average erosion rate that would be appropriate for the different exposure regimes as well as for the different lithologies. With caution, we follow the procedure of other works with regards to this correction and estimate the inevitable increase to our calculated ages for 'reasonable' or representative erosion rates. Assuming for this calculation that the ^{10}Be concentrations at McLeod and Fisher peaks (the two sites which gave the "oldest" minimum ages) are determined by erosional equilibrium, the mean, long-term erosion rate is 0.18±0.02 mm/ka — a result consistent with other mean erosion rates from previous Antarctic studies [1–5]. Applying this erosion rate to adjust upwards apparent exposure ages causes a 75–220 ka increase for those samples at ~780 m above Battye Glacier (BG-2 to BG-5), and a minor 2–5 ka increase for the older samples (RL-2, 3, 5, 6) at Radok Lake.

Table 2
^{10}Be and ^{26}Al exposure ages from Fisher Massif, Battye Glacier and Radok Lake basin, Amery Oasis, northern Prince Charles Mountains, Antarctica

No.	Sample name	Alt (m)	^{10}Be (atoms/g-Q) ($\times 10^6$) [a]	^{26}Al (atoms/g-Q) ($\times 10^6$) [a]	Scaling factor [b]	Site production rate (at/g/yr) [c]	^{10}Be minimum exposure age (ka) [d]	^{26}Al minimum exposure age (ka) [d]
Fisher Massif								
1	FM-1	1260	27.11±0.63	109.5±5.4	3.876	19.77	2163±241	2311±770
	FM-1-R	1260	26.79±0.62	95.3±4.5	3.876	19.77	2119±233	1535±307
2	FM-2	1187	9.33±0.26	52.6±2.8	3.649	18.61	570±44	620±76
	FM-2-E	1187	9.07±0.22	–	3.649	18.61	551±41	
Battye Glacier								
3	BG-1	1200	23.92±0.57	–	3.689	18.81	1909±199	
4	BG-2	803	10.15±0.38	–	2.620	13.36	934±83	
5	BG-3	782	9.54±0.29	–	2.571	13.11	885±74	
	BG-3-E	782	9.35±0.25	–	2.571	13.11	863±70	
6	BG-4	771	7.64±0.23	–	2.546	12.98	686±55	
	BG-4-R	771	7.59±0.20	33.4±1.6	2.546	12.98	680±53	545±62
7	BG-5	771	6.48±0.22	–	2.546	12.98	567±45	
Radok Lake								
8	RL-1	216	0.518±0.018	2.49±0.25	1.501	7.66	68.8±4.9	54.7±7.1
9	RL-2	212	0.680±0.020	5.50±0.29	1.495	7.63	91.1±6.3	(126±12)
10	RL-3	212	0.895±0.023	10.81±0.60	1.495	7.63	120.6±8.2	(264±27)
11	RL-4	203	0.210±0.011	2.61±0.27	1.482	7.56	27.9±2.2	(58.2±7.6)
12	RL-5	197	0.852±0.053	–	1.473	7.51	116.5±10.4	
13	RL-6	197	0.753±0.034	–	1.473	7.51	102.9±8.0	
14	RL-7	197	0.205±0.027	–	1.473	7.51	27.4±3.9	
15	RL-8	125	0.108±0.004	0.65±0.09	1.367	6.97	15.5±1.1	15.3±2.4
16	RL-9A	123	0.149±0.010	0.77±0.09	1.364	6.96	21.7±1.9	18.2±2.4
	RL-9B	123	0.138±0.014	0.89±0.08	1.364	6.96	19.9±2.2	21.2±2.4
17	RL-10	70	0.073±0.004	0.41±0.04	1.290	6.58	11.1±0.9	10.4±1.2

[a] Concentrations at site location. Uncertainty represents quadrature addition of 1σ errors in final AMS isotope ratio, masses, Al assay and a 2% systematic variability in repeat measurement of AMS standards [32].
[b] Altitude and latitude scaling factors, including modifications for Antarctic pressure–altitude relationship, from Stone [40].
[c] Site production rate based on sea-level, high latitude spallogenic plus muon (2.5%) production rates of ^{10}Be=5.1±0.3 atoms/g/y and ^{26}Al=31.1±1.9 atoms/g/y from Stone [40]. Production corrections for a constant sample thickness of 4 cm shifts ages upwards by ~4–6% (using Λ=150 g/cm^2 and ρ=2.7 g/cm^3). Corrections for both horizon shielding and paleo-geomagnetic field variations were not applicable.
[d] Weighted mean age from individual isotope ^{10}Be and ^{26}Al ages. Uncertainties propagated from concentrations with additional errors of 7% in production rate. ^{26}Al ages shown in ( ) were considered anomalous and rejected.

For ten of the samples we were successful in obtaining paired ^{26}Al and ^{10}Be exposure ages. In all but 3 cases (RL-2, RL-3 and RL-4), the independent ^{26}Al age supports the ^{10}Be result within their 1-σ total age error indicating non-complex or continuous exposures. Two cases (FM-1-R, BG-4-R) differ in their ^{10}Be and ^{26}Al ages by between 1- and 2-σ, leading to possible scenarios explained by a complex history of pre-exposure, burial and subsequent re-exposure. For RL-2 agreement is seen only at the full 2-σ error range. However, for RL-3 and RL-4 we are unable to explain the factor of two *larger* ^{26}Al exposure age compared to their paired ^{10}Be result. Repeat AMS measurements of these 2 targets did not identify any issues relating to ^{26}Al identification, or stable ^{27}Al ion current determination. No residual HF solution was available to confirm their native Al concentration by repeat ICP-AE measurement. We are unable to provide a reasonable explanation for such a result and omit these 3 ages from the following discussions.

The ^{10}Be ages spread considerably – by a factor of 200 from 10 ka to 2 Ma – across the 1200 m altitude range sampled. They appear to bracket into 3 (minimum) age groups associated with their altitudes; those at 2 Ma from peaks of Fisher and McLeod Massifs, those from 0.6 to 0.9 Ma above Battye Glacier and those <0.12 Ma from the North Arm of Radok Lake. The correlation of decreasing apparent (minimum) exposure age with lower altitude is given in Fig. 4 with focus on samples from Radok Lake. Even within a given location where altitude differences between adjacent samples are negligible, a

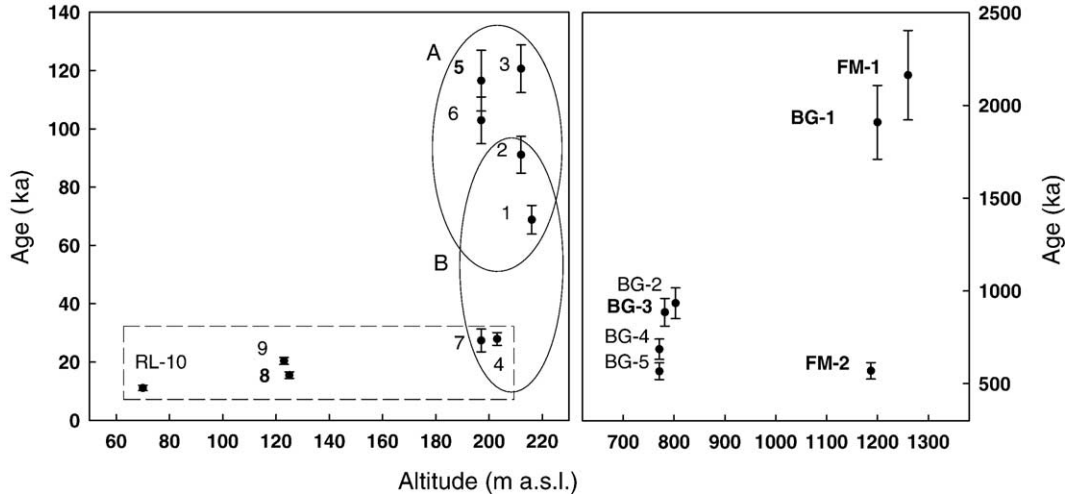

Fig. 4. ^{10}Be exposure ages against altitude (above sea-level) for all samples (bold sample numbers denote bedrock or tors). The left panel shows data from Radok Lake with those at ~220 m above North Arm grouped via ellipses into 2 process dependant categories viz. (A) representing ages altered via inheritance and alternatively (B) ages altered by post-depositional production rate reduction. Given (A), the dashed square would then enclose samples representing a single Battye ice advance (at 28 ka) with subsequent deglaciation, while given (B) the data set represents two Battye ice advances, at 120 ka and then at LGM (~20 ka).

comparatively smaller, but significant spread in exposure age persists.

5. Discussion

These intra-site age variations can be understood by considering the various site-dependent processes which alter or skew model dependent age distributions obscuring the association of an 'average age' with the true timing of ice volume change or landform modification by ice [43–45]. Numerous post-depositional geomorphic processes – such as boulder exhumation through overlying till [46,47] or glacial debris flows [48], moraine degradation leading to re-orientation of the boulder surface [49], cover by seasonal snow [50] or residual patchy ice, and large-scale rock surface spalling (or periglacial activity) – can reduce mean production rates over intermittent or prolonged periods resulting in depressed or 'younger' boulder ages than that of the ice advance which formed the moraine. The oldest erratic age then best represents ice retreat, and if applicable, younger ages represent a minimum age for moraine stabilization [51]. In contrast, pre-exposed and sub-glacially transported boulders that have escaped sufficient glacial erosion/breakdown, or re-cycling of older moraine material on young moraines (i.e., a more extensive and younger ice advance overriding a proximal but older moraine) can result in (partial) preservation of an inherited cosmogenic inventory leading to 'apparent exposure ages' older than that of moraine formation [52]. In general these issues have been invoked, with supporting field evidence, in numerous studies of alpine-type deglaciation systems where age spreads may typically be in the range of a few tens of percent (i.e., from 1 to 3σ). Ages outside an 'acceptable' range are usually then referred to as outliers and rejected.

However, more recent works have identified moraines and bedrock surfaces from older glacially moulded formations, which although demonstrably overridden by the most recent ice sheet advance or affected by outlet glaciers at ice-sheet margins, remain intact and undisturbed [45,53–55]. In such cases, ice-abraded bedrock surfaces give exposure ages far older than erratics upon which they have been deposited — whereas in alpine settings, where erosive powers of wet-based ice are high, and an assumed >2 m of bedrock is scoured by ice advance, bedrock and erratic ages would then be coeval. Preservation of prior exposure on bedrock can lead to a quantitative estimate of the degree of sub-glacial erosion or plucking [56]. In addition, under cold-based ice sheet conditions, storage, reworking and recycling of sub-glacial transported rocks, can deliver erratics with a higher proportion of inheritance than that observed in alpine settings. For both latter scenarios, young erratic ages, particularly if lower than bedrock ages, may well represent the timing of deposition by ice [14]. These issues are considered in interpreting our intra-site exposure age variations.

5.1. McLeod Massif and Battye Glacier escarpment

The 5 samples from this region (Figs. 3 and 4 right-hand panel) have minimum ^{10}Be exposure ages ranging from close to the Pliocene–Pleistocene boundary to mid Pleistocene. The oldest sample (BG-1) at 1909±199 ka is from the summit of an unnamed 1200 m peak on the crest of McLeod Massif whereas the remaining 4 samples (BG-2 to BG-5) range in age between ca. 900 and 550 ka, and are located at altitudes of 770 to 800 m on top of the escarpment overlooking Battye Glacier (Fig. 3). As such, these 5 ages document the emergence of McLeod Massif from beneath the EAIS since the early Pleistocene. This episode of deglaciation considerably postdates deposition of the mid-Miocene Battye Glacier Formation nearby at Dragons Teeth but broadly compares with, or is only slightly younger than, the deposition of the late Plio–Pleistocene Bardin Bluffs Formation ca. 1.0–2.6 Ma [57] 9.5 km to the southeast across the Amery Fault.

BG-2, at 803 m, is from a large erratic (1.5 m in height) lying on Pleistocene gravel, while BG-3, nearby at 782 m, is from a bedrock tor (~2 m in height) standing near the escarpment edge. Their equivalent exposure ages of 934 and 885 ka, respectively, indicates that any cosmogenic nuclide concentration inherited previous to the deposition of BG-2 has been effectively removed. The remaining two samples, BG-4 and BG-5, at only 11 m lower altitude, have a lower exposure ages of 686 and 567 ka, respectively. These samples (~0.5 m) were collected from (i) a boulder or erratic lying on fluvial gravels that form an incomplete thin (<1m) blanket on the floor of a shallow northeast trending (fluvial) gully beheaded by the escarpment of Battye Glacier trough and (ii) a boulder from the river gravels directly underneath BG-4. These gravels clearly display ripple and dune bedforms.

Based on the local geomorphic setting, we suggest that these two younger ages (relative to BG-2 and -3) result from both samples, given their 11 m altitude difference, were shielded whilst variably buried within the once much thicker but now largely eroded fluvial gravels. The difference in average ^{10}Be concentrations given in Table 2 between these two pairs of samples can be used to estimate that a *mean* burial depth of only 20 cm would support this assumption. Whilst the exposure age for BG-4 of 686 ka in Table 2 represents the maximum cumulative surface exposure time possible, burial episodes could occur with an initial ~220 ka at large depth (~2 m i.e. height of tor) or intermediate burial, say at 75 cm for an initial 300 ka and final 575 ka of surface exposure. Effectively, all such scenarios of burial and exhumation, would require a process of surface disturbance (i.e. meltwater activity, deflation) or persistence of thicker patchy ice within the paleo-fluvial channels at some time after the site became ice free. That (fluvial gravel) BG-5 has an appreciably younger age (567 ka) than the immediately overlying (boulder or erratic) BG-4 (686 ka) is compatible with the latter having also in part shielded the former. Differential erosion could also explain the age difference if BG-4 and -5 experienced a factor of 2 enhanced erosion rate (i.e. 0.4 mm/ka instead of the 0.2 mm/ka equilibrium erosion rate determined from BG-1 (see above)). The only ^{26}Al exposure age available for this sample set is 545 ka for BG-4-R, which, although overlaps the corresponding ^{10}Be age of 680 ka at the 1σ limit, is consistent with negligible pre-exposure, though some degree of burial cannot be fully ruled out.

Both O'Brien [28] and Theissen et al. [58] noted major changes in Prydz Channel Fan sediment composition and a ten-fold reduction in accumulation rate from ODP core 1167 occurring some time between the Brunhes–Matuyama Boundary (0.78 Ma) and 1.13± 0.35 Ma (based on a strontium isotope date on planktonic forams). They noted a significance change in the dominance of debris flow and sub-glacial melt-out material sourced from erosion of the Lambert Graben prior to ~1.1 Ma to basement-derived lithologies and sedimentary detritus indicative of supply from more coastal ice sites in the younger core sections. Their 10-fold reduction in sedimentation rate from Pliocene to mid-Pleistocene times resulted from an over-deepened Lambert Graben reducing the ability of major Lambert ice-streams to reach the shelf edge since 1.1 Ma ago [59]. An inference made from this observation was a parallel reduction in interior ice accumulation, increased coastal precipitation and subsequent lower ice volume through the Lambert. Our erosion-corrected exposure ages for BG-2 and BG-3 (1.05–1.17 Ma) adds further support and time constraint to these observations from Prydz Bay ODP 1167 sediment studies [28,58] that a major shift in the climatic regime of the region and re-distribution of ice supply to the Amery Shelf occurred ~1.1 Ma ago. Based on our ^{10}Be ages for surfaces at 800 m overlooking Battye Glacier at McLeod Massif, we estimate an ice thickness reduction equivalent to 400 m occurred ~1.05 to 1.17 Ma, and that the peak of Mcleod Massif first emerged above the ice sheet at least 1.91 Ma ago. Uplift by crustal rebound during ice sheet thinning would tend to make a 400 m reduction in thickness a maximum estimate.

5.2. Radok Lake basin

With decreasing altitude, the ten samples (RL-1 to -10) from above the northern and eastern shores of Radok Lake range in age from 121 to 11 ka (Fig. 3). Collectively these ages document the more recent Late Pleistocene glacial history of Battye Glacier ice into Radok Lake basin. Samples RL-1 to RL-7, (197 to 216 masl), vary in age from 121 to 28 ka. RL-8 to RL-10, at lower altitudes, 125 and 70 masl, range in age from 22 to 11 ka. Two samples (RL-5, RL-8) are of Amery Group bedrock from which the Pagodroma Group mantle has been swept clear. The remaining eight samples are either ice-transported erratics deposited when Battye Glacier ice last reoccupied the basin or reworked and exhumed basement boulders derived from the Pagodrama Group when upon overtopping the basin, ice variably eroded the western margin of the Bardin Bluffs Formation of the Pagodroma Group and in places removed it entirely to expose the Amery Group bedrock (e.g. sample RL-5). The overall sub-angular to angular character and larger size of these boulders which protrude distinctly above the gentle sloping but otherwise flat surface, in contrast to the generally sub-rounded and smaller clasts of the Bardin Bluffs Formation, leads us to prefer the former interpretation.

In Fig. 4, left-hand panel, we show age versus altitude for the RL samples. The Radok Lake glacial chronology based on these apparent ages depends largely on the interpretation attributed to two pairs of samples, viz., the apparent young erratics RL-4, -7 and the apparent older bedrock–erratic pair RL-5, -3 as outlined in the following section.

For the higher altitude group of seven samples we assume, given their relative proximity to each other and only 19 m difference in altitude, that they all share a broadly similar depositional history, despite their factor of 4 spread in age. There are numerous scenarios of combinations of erosion, exhumation, inheritance and burial acting over episodic or gradual timescales that could produce these apparent cosmogenic exposure ages as described above. For brevity and to highlight the issue, we present two end-members of possibilities each associated with a plausible and dominant glacio-geomorphic process. First, we consider that the cluster of 3 oldest Pleistocene ages based on erratics RL-3, RL-6 and in particular bedrock RL-5, with an apparent age spread from 103 to 120 ka (mean 115±5 ka) represents our best estimate of continuous exposure and hence timing of a major advance of Battye Glacier ice to a thickness ~220 m above the present-day lake level. Inclusion of an erosion correction (using 0.18 mm/ka) would extend this mean age by at most 5 ka, whilst inclusion of RL-2 (91 ka) lowers the mean to 104±7 ka. This argument requires that (a) *all* other lower apparent ages for the remaining samples (i.e. group B in Fig. 4) are the result of post-depositional production rate decreases due to either partial burial with exhumation, ice shielding or non-uniform rock wastage, (b) ice advance was sufficient in sub-glacial erosive strength to remove any initial cosmogenic inventory in bedrock sample RL-5 and (c) inheritance in derived boulders or transported erratics is negligible or at least not evident in the oldest ages. Both RL-3 and -6 are small cobble-like samples which, following sub-glacial transport, would make them the more likely candidate to retain a minimal, if any, inheritance signal. The 'younger' sample pair, RL-4 and RL-7 (28 ka), would then have undergone a considerable fraction of time (partially) buried within the reworked Pagodroma till drape. As an example, this could be either continuous burial over the full 120 ka period by about 80 cm, or initial burial by 110 cm then exhumation at LGM times, 10–12 ka ago. Clearly such episodic examples are only extreme cases, and tend to give the scale of depth and time required to achieve the measured ^{10}Be concentration that is equivalent to an apparent age of 28 ka. The more likely behavior of slow emergence with removal of overlying debris/sediment would still require that the dominant process to be burial. If not burial, then a boulder surface erosion rate of 19 mm/ka over the 120 ka exposure period (or spalling of a similar total depth) would give the measured RL-4 and -7 concentrations. Comparison with the mean estimated rates of 0.1–0.2 mm/ka for this site and rock type would seem to make this option unlikely.

In contrast, an alternative and equally plausible argument is to assume that these 2 youngest ages represent the best case for minimum influence of cosmogenic nuclide inheritance and thus represent the maximum time for ice at 220 m above Radok Lake. All other older apparent ages (group A in Fig. 4) are the result of either preservation of older reworked basement deposits or incomplete subglacial erosion of entrained erratics during transport. For both cases, this advance of Battye Glacier would necessarily have been cold-based in order to preserve overridden older landforms, prevent bedrock scouring (i.e. RL-5 bedrock sample) and/or deliver debris with a high degree of preservation of original pre-exposed surfaces. Hence if this scenario is correct, then the full compliment of all ages, from 220 to 70 m is the result of Battye glacier fluctuations with a recent maximum ice volume increase at 28 ka (220 m) at LGM times and subsequent continual deglaciation

through the last interglacial to 11 ka (70 m) (i.e. the dashed box in Fig. 4). In effect, cosmogenic dating on its own cannot clearly distinguish between the two arguments presented here.

Independent glacio-geomorphic evidence is also unable to constrain the timing of the last Battye ice advance through Radok lake. Hambrey et al. [unpublished data, [60]] documented periglacial (polygon, tafoni) features and minor melt channel gullies over the clast-rich unconsolidated sediment surface from which samples were taken. This could allow surface modification and exhumation to support the former argument — however note is also made that since Late Pleistocene times, cold-based Battye ice advances were more likely which could well support the later argument. A $\delta^{18}O$ record from ODP core 1167 [28,58] showed as few as three glacial–interglacial cycles can tentatively be assigned to MIS 16–19 between the B/M boundary (~32 mbsf) and a 37 ka ESR-dated foram horizon at 0.45 mbsf. However data are absent for younger core sediments and an unconformity in ODP 1167 between 4 and 6 mbsf prevents any conclusion to be drawn from it regarding EAIS-related ice thickness changes based on our record at Radok Lake over the past 120 ka.

Domack et al. [61] and Taylor and Leventer [62] presented (uncalibrated) radiocarbon ages in Prydz Bay glacial sediments interrupted by marine episodes at >33,590 and at ca. 22,170 BP. The latter age seems unlikely to reflect Battye glacial ice invasion of Radok at 28 ka unless these samples (RL-4 and -7) also contain an inheritance component equivalent to ~4 ka of exposure, whilst the former ^{14}C age may be in part be correlative with the withdrawal of ice from the Radok Lake basin after ~120 ka.

Of the lower altitude group (samples RL-8 to RL-10), paired ^{10}Be and ^{26}Al exposures ages range from 20.4± 1.2 ka (weighted mean for 9A and 9B) to 10.9 ka at altitudes of 123 and 70 masl, respectively. We interpret these ages as documenting the final withdrawal southwards of a much reduced Battye Glacier during the last glacial–interglacial transition. Both RL-9 and RL-10 erratics are from the thrust–moraine complex referred to previously. The documented relict shorelines at Radok Lake [17] range up to ~70 m above today's lake level to a similar elevation to that of RL-10. These features clearly record lowering lake levels during the Holocene as the Battye Glacier receded southwards. Bedrock sample RL-8 located ~7 km further to the south (Fig. 3) at 125 m has an exposure age of 15.4 ka. This sample is from an ice-striated bench of Amery Group strata swept clean of Pagodroma Group deposits. The locality, situated as it is directly opposite the mouth of Battye Glacier valley, records an ancestral floating Battye Glacier tongue that, facilitated by a then higher lake surface, extended across the Radok basin and onto the edge of Dart Fields (Fig. 3). There the grounded ice front eroded the western margin of the Pagodroma Group blanket.

5.3. Fisher Massif

Located some 75 km to the south of Amery Oasis, the 30 km long Fisher Massif (Fig. 1) lies on the western flank of the LG-AIS drainage system. Erosion residuals of two Pagodroma Group formations, namely the mid-Miocene Fisher Bench and the lower Miocene or Oligocene Mount Johnston Formation mantle the massif's Proterozoic basement [23].

Basement samples FM-1 (granodiorite) and FM-2 (quartz vein) from a glacial erosion surface at 1260 and 1187 masl, respectively, from Blustery Cliffs at the northern end of Fisher Massif, provide contrasting ^{10}Be exposure ages of 2163 and 570 ka, respectively (Table 2). Their concordant ^{26}Al ages support each to have had a continuous, but widely different, period of exposure.

The 2.2 Ma mean (minimum) apparent age for FM-1 (the oldest within the entire set), demonstrates that Fisher Massif emerged from beneath ice cover in the late Pliocene and to have been then continuously exposed. However, the repeat ^{26}Al age of 1535 ka for FM-1-R, although within 1-σ of FM-1, could be considered to be discordant with both ^{10}Be ages. We resist the option to invoke a complex burial history for Fisher Massif based on this younger ^{26}Al age without additional samples to verify this approach. We note that for such large ^{26}Al ages, a 5% increase (i.e. ~1σ) in the stable Al assay (equivalent to +4 μg/g for FM-1-R) would result in a 15% age increase. As the grounding-line of the Lambert Glacier is ~150 km further to the south, in the vicinity of Mt Stinear, the depositional bathymetry of the Pagodroma Group is not yet known, and hence a minimum uplift in excess of 1200 m for FM-1 is to be contemplated. Consequently, FM-1 reveals little of the ice sheet's late Pliocene surface altitude. However, we make the observation that the 2.2 Ma (minimum) exposure age at today's 1260 m altitude for Fisher peak is similar to the 1.9 Ma exposure age of BG-1 at McLeod Massif peak at the similar altitude of 1200 masl.

Sample FM-2 is from a quartz vein within fissile and easily erodable metasediments closely adjacent to the granodioritic pluton from where FM-1 was sampled. On the two assumptions that both sites emerged together through a receding ice sheet surface about 2 Ma and that both remained continuously exposed without being

subsequently overridden (according to their concordant ^{26}Al ages), we attribute the much younger age of sample FM-2 to either some form of complete and prolonged shielding by ice, rock or glacigenic sediment or that its cosmogenic signal was largely reset. We draw on two simple scenarios — deep coverage by local or cirque ice (>~10 m) shielded our sample and this persisted until 0.5 Ma ago or that bedrock removal of the order of at least a few m occurred rapidly at that time. Whichever scenario is taken, sample FM-2 certainly did not undergo a history of initial exposure, followed by a period of burial under ice and then re-exposure, as no burial signal is evident from its paired ^{10}Be and ^{26}Al age (i.e., a ^{26}Al/^{10}Be ratio of 5.6±0.4).

6. Conclusions

Exposure ages in the Amery Oasis region of the northern Prince Charles Mountains record major periods of ice volume reduction for this sector of the East Antarctic Ice Sheet. The interval covered is from the Pliocene–Pleistocene boundary to the beginning of the Holocene spanning a broad time period from 2163 to 11 ka. The ages cluster into three groups that decrease in age with both decreasing altitude (from 1260 to 70 masl) and increasing proximity to the Lambert Glacier–Amery Ice Shelf drainage system. This provides for the first time an absolute chronological framework of Quaternary deglaciation events that is consistent with, and underpins, previous geomorphic studies of the Lambert Graben region. We summarize our conclusions as follows:

(1) Proterozoic basement rocks at the peaks of McLeod (now at 1200 masl) and Fisher Massif (1260 m) first emerged above the surface of the Mac.Robertson Land lobe of the East Antarctic Ice Sheet at least 1.9 and 2.2 Ma, respectively and have been continuously exposed since that time.
(2) Ice volume reduction continued during the mid-Pleistocene with lower altitude (~800 m) plateau features below McLeod Massif peak and adjacent to Battye Glacier, becoming ice-free at 1.15 Ma based on erosion-corrected exposure ages. This correlates with a major marine depositional event at 1.13 Ma [28,58] in Prydz Bay Channel Fan ODP core 1167. Moreover, this boundary defines a significant change in climatic conditions (from δ^{18}O), accumulation rates and dynamic ice flow regimes whereby older (>1.1 Ma) ice erosion events [28] are represented by debris flows resulting from ice of the Lambert–Amery system reaching the shelf break, whilst younger (<1.1 Ma) core sections indicate ice delivery from more coastal sites. This evidence indicates that ice incursion to Radok Lake basin after the mid-Pleistocene Transition ~1 Ma ago [58] may not be representative of ice volume changes in Lambert Glacier flow.
(3) Radok Lake basin was reoccupied by a major re-advance of Battye Glacier ice to ~220 m above today's lake surface within the last glacial cycle either at 28 or 120 ka (i.e. between MIS 2 and 5) — the choice being dependent on interpretation of exposure ages from samples at the maximum and minimum spread in ages from the North Arm of Radok Lake. If this last major Battye ice incursion was at 28 ka, then cold-based ice flow is required at least at ice-marginal sections. The age of the initial excavation of Radok Lake basin is not yet known.
(4) Battye Glacier withdrew from the northernmost shores of the basin's North Arm at ~11 ka, indicating that the most recent period of ice reduction in the Amery Oasis occurred at local LGM times.

Acknowledgments

This work was supported by AINSE grant 025/96, ASAC grants to B.C.M and ARC grant A00/000967 to D.F. Funding and generous support from ANSTO for Project OP-0203v is acknowledged. MJH acknowledges support from UK NERC funding. We thank Charles Mifsud and David Child at ANSTO for their contribution in sample processing.

References

[1] K. Nishiizumi, C.P. Kohl, J.R. Arnold, J. Klein, D. Fink, R. Middleton, Cosmic ray produced ^{10}Be and ^{26}Al in Antarctic rocks: exposure and erosion history, Earth Planet. Sci. Lett. 104 (1991) 440–454.
[2] E.J. Brook, M.D. Kurz, R.P. Ackert Jr, G.H. Denton, E.T. Brown, G.M. Raisbeck, F. Yiou, Chronology of Taylor Glacier advances in Arena Valley, Antarctica, using in-situ cosmogenic ^{3}He and ^{10}Be, Quat. Res. 39 (1993) 11–23.
[3] E.J. Brook, E.T. Brown, M.D. Kurz, R.P Ackert Jr, G.M. Raisbeck, F. Yiou, Constraints on age, erosion, an uplift of Neogene glacial deposits in the Transantarctic Mountains derived from in-situ cosmogenic ^{10}Be and ^{26}Al, Geology 23 (1995) 1063–1066.
[4] L.A. Bruno, H. Baur, T. Graf, C. Shlucter, P. Signer, R. Weiler, Dating of Sirius Group Tillites in the Transantarctic Mountains with cosmogenic ^{3}He and ^{21}Ne, Earth Planet. Sci. Lett. 147 (1995) 37–54.
[5] S. Ivy-Ochs, C. Schluchter, P.W. Kubik, B. Dittrich-Hannen, J. Beer, Minimum ^{10}Be exposure ages of early Pliocene for the

Table mountain Plateau and the Sirius Group at Mt Fleming, Dry Valleys, Antarctica, Geology 23 (1995) 1007–1010.
[6] J.M. Schaefer, S. Ivy-Ochs, R. Weiler, I. Leya, H. Baur, G.H. Denton, C. Schluchter, Cosmogenic noble gas studies in the oldest landscape on earth: surface exposure ages of the Dry valleys, Antarctica, Earth. Planet. Sci. Lett. 167 (1999) 215–226.
[7] D.E. Sugden, M.A. Summerfield, G.H. Denton, T.I. Wilch, W.C. McIntosh, D.R. Marchant, R.H. Rutford, Landscape development in the Royal Society Range, southern Victoria land, Antarctica, Geomorphology 28 (1999) 181–200.
[8] G.H. Denton, D.E. Sugden, D.R. Marchant, B.I. Hall, T.I. Wilch, East Antarctic sensitivity to Pliocene climate change from a Dry valley perspective, Geogr. Ann. V75A (1993) 155–204.
[9] B.C. McKelvey, P.N. Webb, D.M. Harwood, M.C.G. Mabin, The Dominion Range Sirius Group — a record of Late Pliocene–early Pleistocene Beardmore Glacier, in: M.R. Thompson, J.A. Crane, J.W. Thompson (Eds.), Geological Evolution of Antarctica, Cambridge University Press, 1991, pp. 675–682.
[10] P.N. Webb, D.M. Harwood, Late Cenozoic history of the Ross Embayment, Antarctica, Quat. Sci. Rev. 10 (1991) 215–223.
[11] G.S. Wilson, The Neogene East Antarctic ice sheet; a dynamic or stable feature, Quat. Sci. Rev. 14 (1995) 101–123.
[12] C.J. Fogwill, M.J. Bentley, D.E. Sugden, A.R. Kerr, P.W. Kubik, Cosmogenic nuclides ^{10}Be and ^{26}Al imply limited Antarctic ice Sheet thickening and low erosion in the Shackelton Range for >1 My, Geology 32 (2004) 265–268.
[13] P. Oberholzer, C. Baroni, J.M. Schaefer, G. Orombelli, S. Ivy-Ochs, P.W. Kubik, H. Baur, R. Weiler, Limited Plio–Pleistocene glaciation in Deep Freeze Range, northern Victoria Land, Antarctica, derived from in-situ cosmogenic nuclides, Antarct. Sci. 15 (2003) 493–502.
[14] J.O. Stone, G.A. Balco, D.E. Sugden, M.W. Caffee, L.C. Sass III, S.G. Cowdrey, C. Cowdrey, Holocene deglaciation of Marie Byrd Land, West Antarctica, Science 299 (2003) 99–102.
[15] D. White, D. Gore, D. Fink, A. Mackintosh, J. Pickard, P. Fanning, B. Ferguson, Constraining the last local glacial maximum in the Lambert Glacier–Amery Ice Shelf system, East Antarctica, abstract only, AGU, Dec 2005; and PhD thesis, unpublished, Dept. of Physical Geography, Univ. of Macquarie, 2006.
[16] K. Lilly, Use of cosmogenic nuclides to constrain the glacial history of the Lambert–Amery Basin, East Antarctica, interim PhD report, Research School of Earth Sciences, ANU, Canberra, Australia, Mar 2005 (internal report, unpublished).
[17] D.A. Adamson, M. Mabin, J.G. Luly, Holocene isostasy and late Cenozoic development of landforms including Beaver and Radok lake basins in the Amery Oasis, Prince Charles Mountains, Antarctica, Antarct. Sci. 9 (1997) 299–306.
[18] V.I. Bardin. Oasis in the ice-bound land. Science in the USSR, No. 4, 1986 86–95, p. 120.
[19] H.M. Stagg, The structure and origin of Prydz Bay and MacRobertson Shelf, East Antarctica, Tectonophysics 114 (1986) 315–340.
[20] M.J. Hambrey, J.A. Dowdeswell, Flow regime of the Lambert Glacier–Amery Ice Shelf system, Antarctica: structural evidence from satellite imagery, Ann. Glaciol. 20 (1994) 401–406.
[21] N.C.N. Stephenson, Geochemistry of granulite-facies granitic rocks from Battye Glacier, northern Prince Charles Mountains East Antarctica, Aust. J. Earth Sci. 47 (2000) 83–94.
[22] S. McLoughlin, A.N. Drinnan, The sedimentology and revised stratigraphy of the Permian–Triassic Flagstone Bench Formation, Northern Prince Charles Mountains, east Antarctica, Geol. Mag. 134 (1997) 335–353.
[23] B.C. McKelvey, M.J. Hambrey, D.M. Harwood, M.C.G. Mabin, P.N. Webb, J.M. Whitehead, The Pagodroma Group — a Cenozoic record of the East Antarctic ice sheet in the northern Prince Charles Mountains, Antarct. Sci. 13 (2001) 455–468.
[24] J.M. Whitehead, B.C. McKelvey, The stratigraphy of the Pliocene–lower Pleistocene Bardin Bluffs Formation, Amery Oasis, northern Prince Charles Mountains, Antarctica, Antarct. Sci. 13 (2001) 79–86.
[25] M.J. Hambrey, B.C. McKelvey, Major Neogene fluctuations of the East Antarctic Ice Sheet: stratigraphic evidence from the Lambert Glacier region, Geology 28 (2000) 887–890.
[26] M.J. Hambrey, B.C. McKelvey, Neogene fjordal sedimentation on the western margin of the Lambert Graben, East Antarctica, Sedimentology 47 (2000) 577–607.
[27] M. Hambrey, W. Ehrmann, B. Larson, Cenozoic glacial record of the Prydz bay continental shelf, East Antarctica, Proc. ODP Sci. Results, vol. 119, 1991, pp. 77–132.
[28] O'Brien et al., Prydz Channel Fan and the history of extreme ice advances in Prydz Bay, in: A. Cooper and P. O'Brien (eds). Proc ODP Sci. Results, vol. 188 (CD-ROM), (2004), College Station, Texas, USA.
[29] C.P. Kohl, K. Nishiizumi, Chemical isolation of quartz for measurement of in-situ-produced cosmogenic nuclides, Geochim. Cosmochim. Acta 56 (1992) 3583–3587.
[30] D. Child, G. Elliott, C. Misfud, A.M. Smith, D. Fink, Sample Processing for Earth Science Studies at ANTARES, Nucl. Instrum. Methods B B17 (2000) 856–860.
[31] D. Fink, M.A.C. Hotchkis, Q. Hua, G.E. Jacobsen, A.M. Smith, U. Zoppi, D. Child, D.C. Mifsud, H.A. van der Gaast, A.A. Williams, M. Williams, The ANTARES AMS Facility at ANSTO, Nucl. Instrum. Methods B223–B224 (2004) 109–115.
[32] D. Fink, B. McKelvey, D. Hannan, D. Newsome, Cold rocks, hot sands: in-situ cosmogenic applications in Australia at ANTARES, Nucl. Instrum. Methods B172 (2000) 838–846.
[33] K. Nishiizumii, ^{10}Be, ^{26}Al, ^{36}Cl and ^{41}Ca AMS Standards, abstract only, Proc. 9th Int. Accelerator Mass Spectrometry Conference, Nagoya, Japan, Sept 9–13, 2002, p. 130.
[34] T.C. Partridge, D.E. Granger, M.W. Caffee, R.J. Clarke, Lower Pliocene hominid remains from Sterkfontein, Science 300 (2003) 607–612.
[35] NIST, 100 Bureau Drive, Stop 1070, Gaithersburg, MD 20899-1070 (www.nist.gov.au).
[36] K.G.W. Inn, S. Raman, B.M. Coursey, J. Fassett, R.L. Walker, Development of the NBS ^{10}Be/^{9}Be isotopic standard reference material, Nucl. Instrum. Methods B29 (1987) 27–31.
[37] H.J. Hofmann, J. Beer, GF. Bonani, H.R Von Gunten, S. Raman, M. Suter, R.L. Walker, W. Wolfli, D. Zimmerman, ^{10}Be: half-life and AMS standards, Nucl. Instrum. Methods B29 (1987) 32–36.
[38] R. Middleton, L. Brown, B. Dezfouly-Arjomandy, J. Klein, On ^{10}Be standards and the half life of ^{10}Be, Nucl. Instrum. Methods B82 (1993) 399–403.
[39] D. Lal, Cosmic ray labeling of erosion surfaces: in situ nuclide production rates and erosion models, Earth Planet. Sci. Lett. 104 (1991) 424–439.
[40] J.O. Stone, Air pressure and cosmogenic isotope production, J. Geophys. Res. -Solid Earth 105 (2000) 23753–23759.
[41] T.J. Dunai, Scaling factors for production rates of in situ produced cosmogenic nuclides: a critical reevaluation, Earth Planet. Sci. Lett. 176 (2000) 157–169.

[42] K. Nishiizumi, E.L. Winterer, C.P. Kohl, J. Klein, R. Middleton, D. Lal, J. Arnold, Cosmic ray production rates of ^{10}Be and ^{26}Al in quartz from glacially polished rocks, Geophys. Res. 94 (1989) 17907.

[43] J.C. Gosse, F.M. Phillips, Terrestrial in situ cosmogenic nuclides: theory and application, Quat. Sci. Rev. 20 (2001) 1475–1560.

[44] G. Balco, J.O.H. Stone, S.C. Porter, M. Caffee, Cosmogenic-nuclide ages for New England coastal moraines, Martha's Vineyard and Cape Cod, Massachusetts, USA, Quat. Sci. Rev. 21 (2002) 2127–2135.

[45] J. Staiger, J. Gosse, J. Johnson, J. Fastook, J. Gray, D. Stockli, L. Stockli, R. Finkel, Quaternary relief generation by polythermal glacier ice, Earth Surf. Process. Landf. 30 (2005) 1145–1159.

[46] M. Zreda, F.M. Phillips, D. Elmore, Cosmogenic ^{36}Cl accumulation in unstable landforms 2. Simulations and measurements on eroding surfaces, Water Resour. Res. 30 (1994) 3127–3136.

[47] R. Zech, B. Glaser, P. Sosin, P. Kubik, W. Zech, Evidence for long-term landform instability on hummocky moraines in the Pamir Mountains (Tajikistan) from ^{10}Be surface exposure dating, Earth Planet. Sci. Lett. 237 (2005) 453–461.

[48] M. Kaplan, N. Hulton, A. Coronato, J. Rabassa, J. Stone, P. Kubik, Cosmogenic Nuclide measurement in southernmost South America and implications for landscape change, in review, Geomorphology (2005).

[49] J. Putkonen, T. Swanson, Accuracy of cosmogenic ages for moraines, Quat. Res. 59 (2003) 255–261.

[50] L. Benson, R. Madole, W. Phillips, G. Landis, T. Thomas, P. Kubik, The probable importance of snow and sediment shielding on cosmogenic ages of north central Colorado Pinedale and pre-Pinedale moraines, Quat. Sci. Rev. 23 (2004) 193–206.

[51] J.P. Briner, D.S. Kaufman, W.F. Manley, R.C. Finkel, M.W. Caffee, Cosmogenic exposure dating of late Pleistocene moraine stabilization in Alaska, Geol. Soc. Amer. Bull. 117 (2005) 1108–1120.

[52] J.P. Briner, D.S. Kaufman, A. Werner, M.W. Caffee, L. Levy, W. Manley, M. Kaplan, R.C. Finkel, Glacier re-advance during late glacial Younger Dryas (?) in the Ahklun Mountains, southwestern Alaska, Geology 30 (2002) 679–682.

[53] J.P. Briner, G.H. Miller, P.T. Davis, P.R. Bierman, M.W. Caffee, Last Glacial Maximum ice sheet dynamics in Artic Canada inferred from young erratics perched on ancient tors, Quat. Sci. Rev. 22 (2003) 437–444.

[54] D. Fabel, A.P. Stroeven, J. Harbor, J. Kleman, D. Elmore, D. Fink, Landscape preservation under Fennoscandian ice sheets determined from in situ produced ^{10}Be and ^{26}Al, Earth. Planet. Sci. Lett. 201 (2002) 397–406.

[55] J. Harbor, A. Steroven, D. Fabel, J. Kleman and D. Fink, Cosmogenic nuclide evidence for minimal erosion across two subglacial sliding boundaries of the late glacial Fennoscandian ice sheet, in press, Geomorphology, Aug 2005.

[56] P. Colgan, P. Bierman, D. Mickleson, M. Caffee, Variation in glacial erosion near the southern margin of the Laurentide Ice Sheet, south-central Wisconsin, USA: implications for cosmogenic dating of glacial terrains, Geol. Soc. Amer. Bull. 114 (2002) 1581–1591.

[57] J.M. Whitehead, B.C. McKelvey, The stratigraphy of the Pliocene–lower Pleistocene Bardin Bluffs Formation, Amery Oasis, northern Prince Charles Mountains, Antarctica, Antarct. Sci. 13 (2001) 79–86.

[58] K. Theissen, R. Dunbar, A. Cooper, D. Mucciarone, D. Hoffman, The Pleistocene evolution of the East Antarctic Ice Sheet in the Prydz Bay region: stable isotopic evidence from ODP Site 1167, Glob. Planet. Change 39 (2003) 227–256.

[59] J. Taylor, M.J. Siegert, A.J. Payne, M.J. Hambrey, P.E. O'Brien, A.K. Cooper, G. Leitchenkov, Topographic controls on post-Oligocene changes in ice-sheet dynamics, Prydz Bay region, East Antarctica, Geology 32 (2004) 197–2000.

[60] M. Hambrey, et al., (manuscript in preparation and private communication (2005).

[61] E. Domack, E.P. O'Brien, P.T. Harris, F. Taylor, P.G. Quilty, L. De Santis, B. Raker, Late Quaternary sediment facies in Prydz Bay, East Antarctica and their relationship to glacial advance onto the continental shelf, Antarct. Sci. 10 (1998) 236–246.

[62] F. Taylor, A. Leventer, Late Quaternary depositional environment in Prydz Bay, Antarctica: preliminary interpretations from marine diatoms, Antarct. Sci. 15 (2003) 512–521.